Available online at www.sciencedirect.com
SCIENCE DIRECT®
International Journal of Solids and Structures 42 (2005) 393–408
INTERNATIONAL JOURNAL OF SOLIDS and STRUCTURES
www.elsevier.com/locate/ijsolstr

Elastic properties of inhomogeneous transversely isotropic rocks

V.M. Levin, M.G. Markov *

Instituto Mexicano del Petróleo, Eje Central Lázaro Cárdenas N152, C.P. 07730 Mexico, DF, Mexico

Received 13 April 2004; received in revised form 14 June 2004
Available online 26 August 2004

Abstract

The problem to determine the effective elastic moduli and velocities of elastic wave propagation in transversely isotropic solid containing aligned spheroidal inhomogeneities (solid grains, vugs and micro-cracks) has been solved using the self-consistent scheme known as effective medium approximation (EMA). Since a solution of so-called one-particle problem is a base for each self-consistent method, we solved this problem as a first step for spheroidal inhomogeneity in a transversely isotropic medium. In contrast to the known solution of this problem by Lin and Mura we obtained the expressions for the strain field inside inclusion in the explicit form (without quadratures). The obtained solution was used then in the symmetric variant of the EMA where each component of the system was considered as spheroid with its own aspect ratio. This approach was applied to simulate the properties of the rocks containing isolated pores and micro-cracks. For connected fluid-filled pores we used the anisotropic variant of the Gassmann theory. The results of the calculations, obtained for the effective elastic moduli, have been compared with the experimental data and theoretical simulations of the other authors. Unlike many other rock mechanics theories, EMA approximation gives correct elastic moduli values even in the nondilute concentration of inhomogeneities. The comparison of the experimental data for oriented crack system with the EMA predictions indicates their good correspondence.
© 2004 Elsevier Ltd. All rights reserved.

Keywords: Effective-medium approximation; Anisotropic elasticity; Elastic wave velocities

1. Introduction

Natural rocks containing inhomogeneities (for example, cracks, cavities or inclusions with other properties) can be considered as micro-inhomogeneous materials. The micro-structure of such materials

* Corresponding author. Tel.: +52 3003 7098; fax: +52 3003 7079.
E-mail addresses: vlevine@imp.mx (V.M. Levin), mmarkov@imp.mx (M.G. Markov).

0020-7683/$ - see front matter © 2004 Elsevier Ltd. All rights reserved.
doi:10.1016/j.ijsolstr.2004.06.044

is random because of the randomness of the shapes and sizes of the inhomogeneities as well as their distribution in space.

As a result, various physical fields in such materials are also random and the central problem of micromechanics is evaluation of the mean values of these fields and relation between them (a homogenization problem). If this problem is solved and such relations are constructed, it is possible to replace the given inhomogeneous medium by a homogeneous one with the effective overall properties of the original material. The responses of such a homogeneous medium and of the original medium to the external loading are macroscopically equivalent.

When the volume concentration (or density) of inhomogeneities is small (so that they do not interact) the homogenization problem is reduced to the problem of an isolated inclusion embedded into a homogeneous matrix. For homogeneous ellipsoidal inclusions and elliptical cracks this problem can be solved exactly, and, therefore, the exact solution of the homogenization problem can be obtained in these cases, see Nur (1971), Anderson et al. (1974), Hudson (1980, 1981, 1990), Peacock and Hudson (1990), Sayers and Kachanov (1991), Kachanov (1992), Thomsen (1995), Cheng (1993) and Xu (1998). For higher inclusion volume concentration, one has to take into account the interaction between them (a many-particle problem), and the homogenization problem becomes much more complex. The many-particle problem for a medium with a random set of inhomogeneities cannot be solved exactly, and only various approximations are available.

In theoretical physics, there is a group of methods known as self-consistent methods, which allow constructing approximate solutions of the many-particle problem. Using physically reasonable hypotheses these methods reduce many-particle problem to the one-particle one. The self-consistent schemes widely used in geomechanics are various versions of the so-called effective medium approximation (EMA) (O'Connell and Budiansky, 1974; Budiansky and O'Connell, 1976; Korringa et al., 1979; Berryman, 1980, 1992; Berge et al., 1993). It is known that this method satisfies the Hashin–Shtrikman bounds and it is realizable (Milton, 1985). The differential scheme (DEM) developed by Norris (1985), Sheng (1991), Berryman (1992), Hornby et al. (1994) and Jacobsen et al. (2000) may be also considered as a version of EMA.

The EMA is based on the following main hypotheses: every inhomogeneity (inclusion) in a micro-inhomogeneous material behaves as an isolated one embedded in a homogeneous medium with effective properties of the original inhomogeneous material. The field action on this inclusion coincides with the external field applied to the material. It is well known that the solution of the homogenization problem based on these hypotheses often does not correspond to experimental data (especially for materials with big contrast in component properties). Nevertheless, for natural rocks this model is preferable in the broad range of cases because of the concept of the critical porosity (Mavko et al., 1998). According to this concept, there is a critical porosity for natural rocks such that when it is exceeded, the rock formation is no longer a connected body (the shear modulus turns to zero). The EMA inability to describe properly the dependence of rock electroconductivity on the total porosity is often referred to its character drawback. But under the appropriate choice of the pores and solid grains geometry, the EMA can also be successfully used for the rock electroconductivity description (Markov et al., 2003).

Based on the EMA, we present the determination of elastic parameters (elastic moduli and wave velocities) of inhomogeneous natural rocks having macroscopically hexagonal symmetry (transversely isotropic). This kind of anisotropy can be caused by aligned spheroidal inclusions (voids or cracks). In this case, the EMA application requires solution of the elastic problem for the isolated spheroidal inhomogeneity in the transversely isotropic medium. With the help of Eshelby's tensor presentation suggested by Vaculenko (1998) and the special tensor basis (Kunin, 1983; Kanaun and Levin, 1994) we have found the solution of this one-particle problem in the explicit form without numerical integration. (Previously this solution was given only in quadratures form by Lin and Mura (1973).) Then we used the obtained solution in the EMA to calculate the effective elastic moduli and velocities of the elastic wave propagation in the

medium containing such inhomogeneities. During these calculations we used the "symmetric" with respect to the components variant of the EMA (Berryman, 1992) for materials that contain inclusions with contrast properties. Each of the components is modeled by spheroids with their own aspect ratios. Note that the obtained solution of the homogenization problem is different from both the solution of Hoenig (1979) and Laws and Brockenbrouth (1987) in which thin crack-like inclusions were only considered and the solution by Hornby et al. (1994). In the last publication the combination of the EMA and the DEM was used for the prediction of the effective elastic properties of anisotropic shales. The shapes of the solid particles and pores in Hornby et al. paper were assumed to be the same.

In the present paper we consider materials with components that can be different in shapes. The calculations are performed for the materials containing oblate spheroids (pores and cracks) as well as prolate spheroids that can model channels in heterogeneous rocks. The existence of such channels is typical for materials with secondary porosity.

The elastic characteristics estimation was performed by the EMA for rocks containing isolated saturated pores without fluid overflow. In the case of connected pore system the effective elastic parameters were initially calculated for dry rocks applying the EMA, and then the hydrodynamic mechanism was taken into account using Gassmann's relations for the elastic moduli of dry and fluid-filled pores (Gassmann, 1951; Brown and Korringa, 1975). These relations are represented in the special tensor basis that allows writing them in the compact and convenient for application form.

The structure of the paper is as follows. The solution of the one-particle problem is given in Section 2. The equations of the EMA for transversely isotropic medium are presented in Section 3. The rest of the paper is dedicated to results of the calculations, their analysis and comparison with the results of the other authors and available experimental data.

2. Single spheroidal inclusion in transversely isotropic medium

Let us consider an unbounded elastic medium with the tensor of elastic moduli C^0, containing a region V with other elastic properties C. The equation of static elasticity in displacements for a medium with inhomogeneity is written in the form:

$$\partial_j C_{ijkl}(x)\partial_l u_k(x) = 0, \quad \partial_i \equiv \partial/\partial x_i, \tag{1}$$

$$C_{ijkl}(x) = C^0_{ijkl} + C^1_{ijkl}V(x), \quad C^1_{ijkl} = C_{ijkl} - C^0_{ijkl},$$

where $V(x)$ is the characteristic function of the region V occupied by inclusion. It was shown by Kunin (1983) that the strain field $\varepsilon_{ij}(x) = \partial_{(i}u_{j)}(x)$ in the medium with inhomogeneity (the parenthesis symbol () stands for the symmetrization procedure over the corresponding indexes) satisfies the integral equation which is completely equivalent to Eq. (1):

$$\varepsilon_{ij}(x) = \varepsilon^0_{ij}(x) + \int_V P_{ijkl}(x - x')C^1_{klmn}\varepsilon_{mn}(x')\mathrm{d}x', \tag{2}$$

$$P_{ijkl}(x) = \left.\frac{\partial^2 G_{ik}(x)}{\partial x_j \partial x_l}\right|_{(ij)(kl)}.$$

Here $\varepsilon^0(x)$ is the external strain field that would be in the medium without inhomogeneity, $G_{ik}(x)$ is the Green function of operator $\partial_j C^0_{ijkl}\partial_l$ for the unbounded medium.

Let the inclusion occupy an ellipsoidal domain V with semiaxes a_1, a_2, a_3. In this case the solution of Eq. (2) can be obtained in the closed form. This fact is based on the remarkable Eshelby's theorem

(Eshelby, 1957): if the external field ε^0_{ij} is homogeneous in the domain V, then the strain field ε_{ij} inside V is also homogeneous and it is determined by the expression

$$\varepsilon_{ij} = A_{ijkl}\varepsilon^0_{kl}, \quad A_{ijkl} = (I_{ijkl} + P_{ijmn}C^1_{mnkl})^{-1}, \tag{3}$$

where $I_{ijkl} = \delta_{i(k}\delta_{l)j}$ is the unit tensor and $\mathbf{P}$ is the tensor with constant components

$$P_{ijkl} = -\int_V P_{ijkl}(x - x')\mathrm{d}x' \tag{4}$$

that depend the shape and orientation of ellipsoid. Note that the tensor $\mathbf{P}$ can be expressed via the known Eshelby's tensor $\mathbf{S}$ as

$$P_{ijkl} = S_{ijmn}(C^0_{mnkl})^{-1}. \tag{5}$$

Let the "host" medium be transversely isotropic and the inclusion be a spheroid with the semiaxes $a_1 = a_2 = a$, a_3 and symmetry axis coincident with the medium symmetry axis. This problem was analyzed by Lin and Mura (1973) where the authors have provided the solution in a quadrature form. We found the solution in a sufficiently compact form without numerical integration. To obtain it we used a special tensor basis introduced by Kanaun and Levin (1994) for a transversely isotropic medium and a specific presentation of tensor P proposed by Vaculenko (1998).

Let us introduce a tensor basis $\mathbf{T}$ with elements, which are defined by the unit vector of symmetry axis m and the orthogonal projector on the isotropy plane θ_{ij}

$$\begin{aligned} &T^1_{ijkl} = \theta_{ik}\theta_{lj}|_{(kl)}, \quad T^2_{ijkl} = \theta_{ij}\theta_{kl}, \quad T^3_{ijkl} = \theta_{ij}m_km_l, \\ &T^4_{ijkl} = \theta_{kl}m_im_j, \quad T^5_{ijkl} = \theta_{ik}m_lm_j|_{(ij)(kl)}, \quad T^6_{ijkl} = m_im_jm_km_l, \end{aligned} \tag{6}$$

where $\theta_{ij} = \delta_{ij} - m_im_j$, δ_{ij} is Kronecker symbol. This tensor basis simplifies operations with fourth-rank tensors for a transversely isotropic medium due to its properties presented in Appendix A.

Tensor $\mathbf{P}$ in (3) can be represented in T-basis in the form

$$\mathbf{P} = P_1\mathbf{T}^2 + P_2\left(\mathbf{T}^1 - \frac{1}{2}\mathbf{T}^2\right) + P_3(\mathbf{T}^3 + \mathbf{T}^4) + P_5\mathbf{T}^5 + P_6\mathbf{T}^6, \tag{7}$$

$$\begin{aligned} &P_1 = \frac{\pi}{2}\sum_{l=1}^{3}(b_l - \gamma_l a_l)J^{(l)}_1, \quad P_2 = \frac{\pi}{2}\sum_{l=1}^{3}(2b_l - \gamma_l a_l)J^{(l)}_1, \\ &P_3 = -\frac{\pi}{2}\sum_{l=1}^{3} c_l(J^{(l)}_1 - \xi^2\gamma_l J^{(l)}_2), \\ &P_5 = \pi\sum_{l=1}^{3}\left[(2b_l - \gamma_l a_l)\xi^2 J^{(l)}_2 - c_l(J^{(l)}_1 - \xi^2\gamma_l J^{(l)}_2) + d_l J^{(l)}_1\right], \\ &P_6 = 2\pi\sum_{l=1}^{3} d_l J^{(l)}_2. \end{aligned} \tag{8}$$

Here the coefficients a_l, b_l, c_l, d_l, γ_l ($l = 1,2,3$) are defined by the matrix elastic moduli and the parameters $J^{(l)}_1, J^{(l)}_2$ depend on the inclusion aspect ratio $\xi = a_3/a$. The explicit expressions for these quantities as well as details of derivation of these formulas can be seen in Sevostianov et al. (this issue) and for completeness are presented in Appendix B.

3. The EMA model for a transversely isotropic medium

We now use the solution of the one-particle problem obtained above in the "symmetric" EMA model proposed by Berryman (1980, 1992) and Norris (1985) for the material with aligned spheroidal inclusions. We assume that material of inclusions may be transversely isotropic with the symmetry axis coincident with the spheroid symmetry axis. Then, for the rth component we can write the expression for the tensor of elastic moduli in T-basis as:

$$\mathbf{C}^r = \frac{1}{2}(C^r_{11} + C^r_{12})\mathbf{T}^2 + 2C^r_{66}\left(\mathbf{T}^1 - \frac{1}{2}\mathbf{T}^2\right) + C^r_{13}(\mathbf{T}^3 + \mathbf{T}^4) + 4C^r_{44}\mathbf{T}^5 + C^r_{33}\mathbf{T}^6. \tag{9}$$

We used here the common Voigt's notation for the five independent elastic moduli of the transversely isotropic medium: C^r_{11}, C^r_{12}, $C^r_{66} = \frac{1}{2}(C^r_{11} - C^r_{12})$, C^r_{13}, C^r_{44}, C^r_{33} $(r = 1, 2, \ldots, n)$.

In consequence with the main hypothesis of the EMA model each component in micro-inhomogeneous material is considered as a spheroid embedded in the homogeneous medium having the overall (effective) properties. The external field that acts on this inclusion is equal to the average field in the region occupied by this inclusion. This leads to the following algebraic equation for the tensor of effective elastic moduli C^*_{ijkl} (see Berryman (1980), Norris (1985)):

$$\sum_r c_r[(C^r_{ijkl} - C^*_{ijkl})^{-1} + P^{*(r)}_{ijkl}]^{-1} = 0. \tag{10}$$

Here c^r is the volume concentration of rth component; tensor $P^{*(r)}$ is obtained from the expressions represented in previous Section and Appendix B in which we had to replace the elastic moduli C^0 by the effective elastic moduli C^*. Index r means that expressions for components of this tensor depend on the aspect ratio of the spheroid that belongs to the rth phase. Tensor C^* also has a transversely isotropic symmetry and can be written in T-basis similar to (9):

$$\mathbf{C}^* = \frac{1}{2}(C^*_{11} + C^*_{12})\mathbf{T}^2 + 2C^*_{66}\left(\mathbf{T}^1 - \frac{1}{2}\mathbf{T}^2\right) + C^*_{13}(\mathbf{T}^3 + \mathbf{T}^4) + 4C^*_{44}\mathbf{T}^5 + C^*_{33}\mathbf{T}^6. \tag{11}$$

The system of algebraic equations for these five effective elastic moduli can be obtained if we write (10) in T-basis and then equate each component to zero in this presentation. This result is

$$\begin{aligned}
&\sum_r \frac{c_r}{\Delta^*_r}\left(\frac{C^r_{11} + C^r_{12} - C^*_{11} - C^*_{12}}{\Delta_r} + P^{*(r)}_6\right) = 0,\\
&\sum_r c_r\left[\frac{1}{2(C^r_{66} - C^*_{66})} + P^{*(r)}_2\right]^{-1} = 0,\\
&\sum_r \frac{c_r}{\Delta^*_r}\left(\frac{C^r_{13} - C^*_{13}}{\Delta_r} - P^{*(r)}_3\right) = 0,\\
&\sum_r c_r\left[\frac{1}{C^r_{44} - C^*_{44}} + P^{*(r)}_5\right]^{-1} = 0,\\
&\sum_r \frac{c_r}{\Delta^*_r}\left(\frac{C^r_{33} - C^*_{33}}{\Delta_r} + P^{*(r)}_1\right) = 0,
\end{aligned} \tag{12}$$

where

$$\Delta_r = (C^r_{11} + C^r_{12} - C^*_{11} - C^*_{12})(C^r_{33} - C^*_{33}) - 2(C^r_{13} - C^*_{13})^2,$$

$$\Delta_r^* = 2\left[\left(\frac{(C_{33}^r - C_{33}^*}{\Delta_r} + P_1^{*(r)}\right)\left(\frac{C_{11}^r + C_{12}^r - C_{11}^* - C_{12}^*}{\Delta_r} + P_6^{*(r)}\right) - \left(\frac{C_{13}^r - C_{13}^*}{\Delta_r} + P_3^{*(r)}\right)^2\right].$$

This system of algebraic equations can be solved numerically. The results of calculations will be presented in the next section.

4. The results of calculations

Let us consider a few examples of calculations applying the described above model.

4.1. Velocity anisotropy in the media containing aligned inclusions

As a first example, let us consider a system of inclusions of two types: platelets particles with aspect ratio 1/20, their properties correspond to clays (see Mavko et al. (1998)), and quasispherical particles, which elastic properties correspond to quartz sandstone. Table 1 shows the elastic waves velocities in the components. Such a medium has anisotropy at the nonzero concentration of each component. Fig. 1 presents how the calculated elastic wave velocities depend on angle between the system symmetry axis and the wave propagation direction. The obtained result analysis shows that the effective media has considerable anisotropy; the elastic wave's velocities difference can exceed 10% depending on the direction of propagation.

As a second example, we consider the calculation of effective velocities in the medium containing fluid-filled inclusions of all types: vugs, horizontally crack-like inclusions and vertical channels. The presence of such a complicated pore system is typical, for example, for carbonate rocks. The calculations were carried out for the medium which properties of the water-saturated limestone embedded at a depth of 2–3 km. The data of the medium elastic properties are presented in Table 2. The concentration of inclusions of all types came to 0.01. Vertical channels were simulated by prolate spheroids with aspect ratio $\alpha = 100$, and crack-like inclusions were modeled by oblate spheroids with aspect ratio $\alpha = 0.01$. Analysis of the calculations (Fig. 2) has shown that in this case the effective medium anisotropy is caused by the presence of crack-like inclusions. The presence of vertical channels at the same concentration of inclusions doesn't lead to considerable anisotropy.

When the aspect ratio of the prolate spheroids exceeds 20, velocities with accuracy of more than 1% correspond to the asymptotical velocity for the ideal cylindrical inclusions with a circular cross-section. To compute the elastic characteristic for circular cylinders we apply the expressions presented in Appendix B.

4.2. Comparison of our results with the Hudson theory

As a third example, let us consider the calculation results for the solid rock, with properties corresponding to the fractured limestone in conditions of natural bedding at a depth of about 2 km. We assume that

Table 1
Common input parameters used to generate Fig. 1

Shale properties	P-wave speed	3750 $\mathrm{m\,s^{-1}}$
	S-wave speed	2000 $\mathrm{m\,s^{-1}}$
	Density	2550 $\mathrm{kg\,m^{-3}}$
Sandstone	P-wave speed	6050 $\mathrm{m\,s^{-1}}$
	S-wave speed	4100 $\mathrm{m\,s^{-1}}$
	Density	2650 $\mathrm{kg\,m^{-3}}$

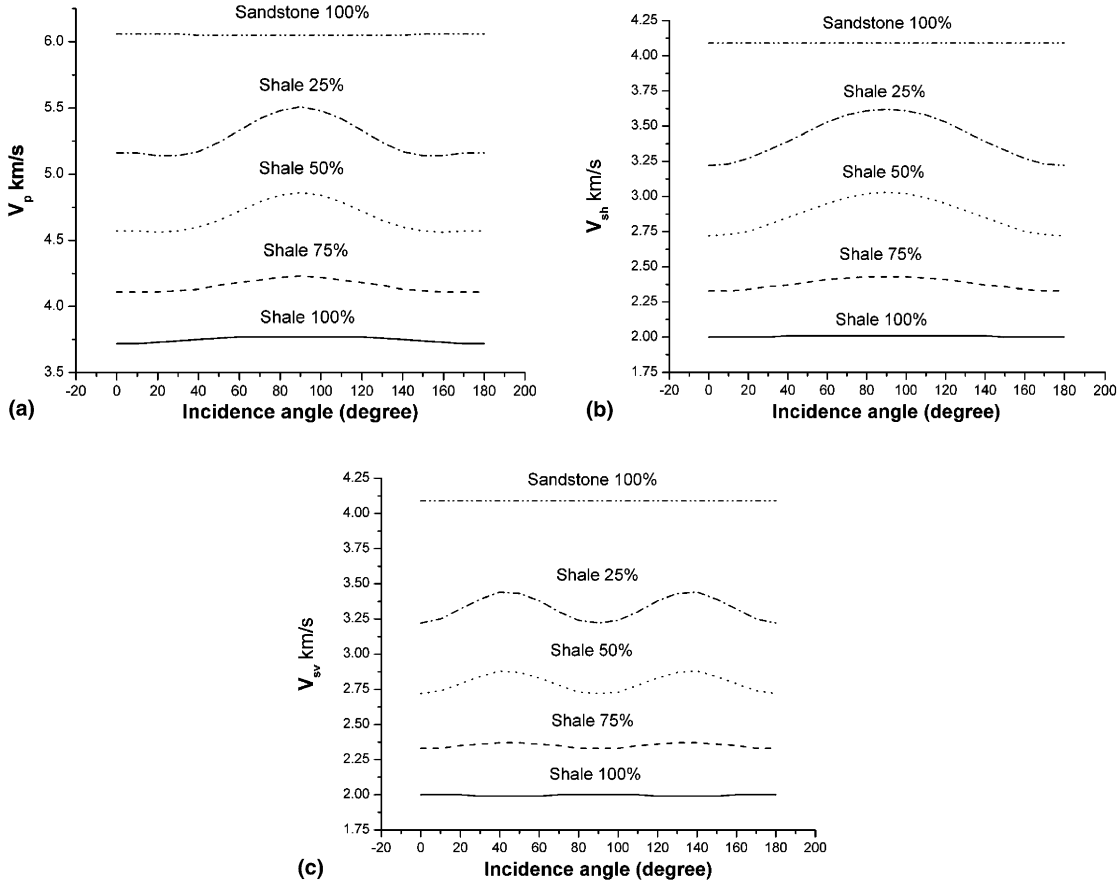

Fig. 1. Velocity dependence on incidence angle in a shale and sandstone mixture (of P-wave (a), SH-wave (b) and SV-wave (c)).

Table 2
Parameters used to generate Figs. 2 and 3

Bulk modulus of the rock	52 GPa
Shear modulus of the rock	27 GPa
Bulk modulus of the pore fluid	2.25 GPa
Crack aspect ratio	0.01
Density	2550 kgm^{-3}

the pores are filled with water; the other rock parameters are shown in Table 2. The dependencies obtained by use of the first-order terms of the Hudson theory (1980) are also presented in Fig. 3. As expected, the obtained results analysis has shown that the Hudson theory and the EMA model are well agreed with each other at the crack density $va^3<0.1$ (the crack concentration < 0.005 for aspect ratio 0.01), where v is the number density of cracks, a is the crack radius. It is necessary to emphasize that this condition is sufficiently strong and don't always fulfill for real rocks. For higher crack concentration it is advisable to use self-consistent methods.

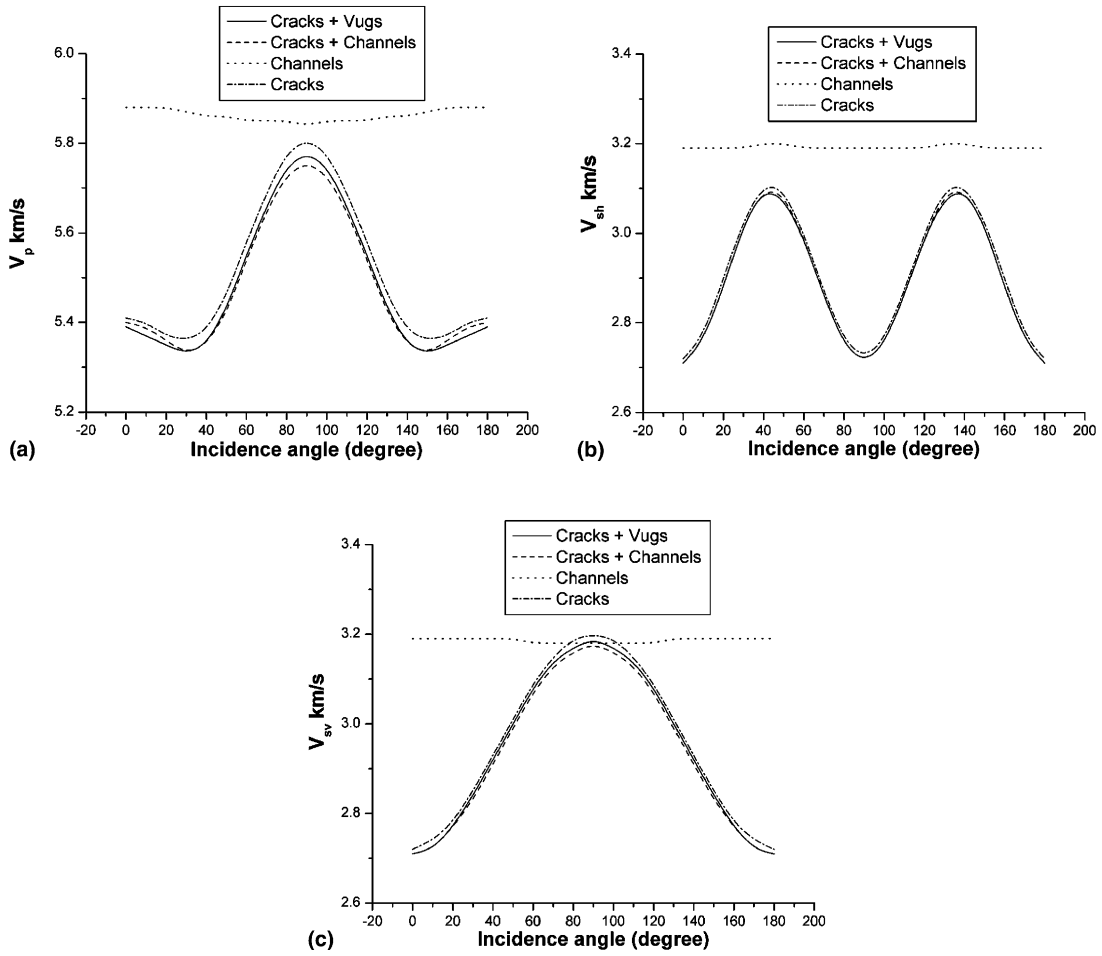

Fig. 2. P-, SH- and SV-wave velocities in a transversely isotropic cracked medium containing components of all forms as functions of incidence angle. Concentration of inclusions of all types is 0.01. The cracks are simulated by spheroids with aspect ratio 0.01, the vertical channels are simulated by spheroids with aspect ratio 100, and the caverns are modeled by spheres.

4.3. Comparison of the calculated P- and S-wave velocities with the experimental data for cracked media

In the paper of Rathore et al. (1994), the measurement results of elastic waves velocities in sandstone containing artificial cracks of given geometry and orientations are represented. The measurements were carried out for saturated and dry samples. The data on the porous matrix and cracks properties are shown in Table 3.

To calculate the elastic wave velocities in cracked media, the following velocity values in dry and wet samples without cracks have been used (Table 4).

In Fig. 4, the calculation results of angle dependencies of V_p-, V_{sh}-, V_{sv}-velocities for the matrix and cracks parameters, corresponding to the experimental data, are shown. The comparison of the experimentally measured dependencies with the predictions indicates their good correspondence. Let us note that in this case, the system of Eq. (6) has a free parameter, aspect ratio, of the first component matrix, but its change in the broad range didn't influence essentially on the obtained dependencies. Fig. 3 is represented

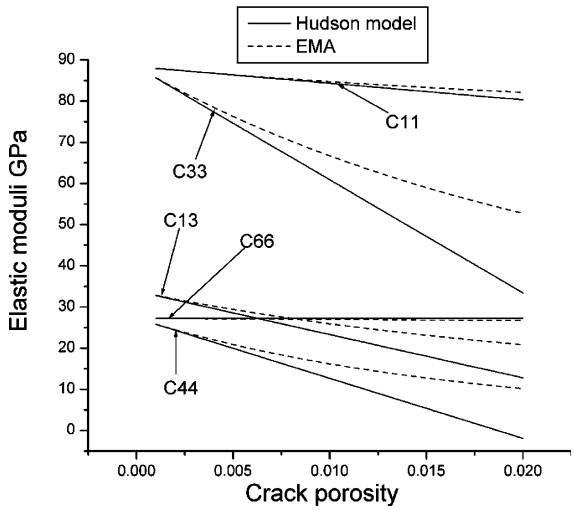

Fig. 3. Comparison of the calculated elastic moduli. Solid lines—Hudson theory, dotted lines—EMA approximation.

Table 3
Crack, fluid and taken from the laboratory experiments of Rathore et al. (1994)

Parameter	Value
Crack half-thickness	10^{-5} m
Crack aspect ratio	0.0036
Crack density	0.1
Fluid bulk modulus	2.16 GPa
Matrix porosity	0.346
Matrix density	1712 kgm^{-3}

Table 4
Velocities in the saturated and dry samples

V_p (dry)	2540 ms^{-1}
V_s (dry)	1440 ms^{-1}
V_p (sat)	2700 ms^{-1}
V_s (sat)	1380 ms^{-1}

for equal aspect ratios of the first type inclusions, corresponding to the matrix without cracks, and the second type inclusions (cracks). For wet samples there is a more complicated situation. In this case the presence of movable fluid in pores and of hydrodynamic cross-flow initiation on the cracks bounds reduces to considerable frequency dispersion of velocities. The most correct account of these effects is possible within the Biot's theory (1962), (Gurevich et al., 1998), however, the complete problem solution of elastic wave propagation in saturated porous media with cracks is beyond the bounds of this paper.

Hudson et al. (1996, 2001) in their works have estimated the influence of hydrodynamic effects, caused by fluid filtration from cracks to pores, on elastic wave velocities and attenuations. Therefore, let us consider only limiting cases, high and low frequencies. Let us emphasize that in this paper we mean by high and low frequencies the frequency value with respect to the typical global (Biot) and local (squirt) flow frequencies,

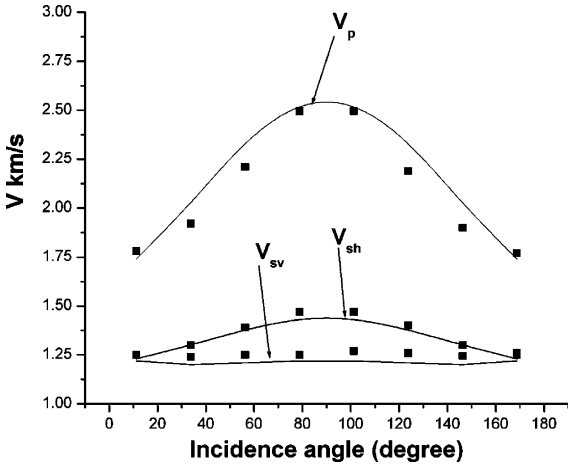

Fig. 4. Comparison of measured data (■) with the EMA model (solid curves) for a dry sample containing micro-cracks.

at the same time the cracks dimension is smaller than the wave length. In our problem definition the EMA model gives the results corresponding to high-frequency approximation Mavko et al. (1998) and considers fluid inclusions as isolated. To calculate elastic module and elastic wave velocities in the low-frequency range we have used relations obtained by Gassmann (1951) and Brown and Korringa (1975). These relations connect the elastic module of dry rock with the elastic module of fluid-saturated rock and are given by:

$$S_{ijkl}^{(\mathrm{dry})} = S_{ijkl}^{(\mathrm{sat})} + \frac{\left(S_{ij\alpha\alpha}^{(\mathrm{dry})} - S_{ij\alpha\alpha}^{0}\right)\left(S_{kl\alpha\alpha}^{(\mathrm{dry})} - S_{kl\alpha\alpha}^{0}\right)}{\left(S_{\alpha\alpha\beta\beta}^{(\mathrm{dry})} - S_{\alpha\alpha\beta\beta}^{0}\right) + (\beta_{\mathrm{fl}} - \beta_0)\phi}, \tag{13}$$

where $S_{ijkl}^{(\mathrm{dry})}$ is the effective elastic compliance tensor for dry rock, $S_{ijkl}^{(\mathrm{sat})}$ is the effective elastic compliance tensor for rock saturated with pore fluid, S_{ijkl}^{0} is the effective elastic compliance tensor for mineral material making up rock, β_{fl} is the pore fluid compressibility, β_0 is the mineral material compressibility, ϕ is the porosity.

The relations (13) in the tensorial basis $T^{(m)}$ are given by:

$$\begin{aligned}
S^{(\mathrm{sat})} &= S_1^{(\mathrm{sat})}T^2 + S_2^{(\mathrm{sat})}\left(T^1 - \frac{1}{2}T^2\right) + S_3^{(\mathrm{sat})}(T^3 + T^4) + S_5^{(\mathrm{sat})}T^5 + S_6^{(\mathrm{sat})}T^6,\\
S_1^{(\mathrm{sat})} &= S_1^{(\mathrm{dry})} - \frac{1}{\Delta_1}\left(2S_1^{(\mathrm{dry})} + S_3^{(\mathrm{dry})} - 2S_1^0 - S_3^0\right)^2,\\
S_2^{(\mathrm{sat})} &= S_2^{(\mathrm{dry})},\\
S_3^{(\mathrm{sat})} &= S_3^{(\mathrm{dry})} - \frac{1}{\Delta_1}(2S_1^{(\mathrm{dry})} + S_3^{(\mathrm{dry})} - 2S_1^0 - S_3^0)(2S_3^{(\mathrm{dry})} + S_6^{(\mathrm{dry})} - 2S_3^0 - S_6^0),\\
S_5^{(\mathrm{sat})} &= S_5^{(\mathrm{dry})},\\
S_6^{(\mathrm{sat})} &= S_6^{(\mathrm{dry})} - \frac{1}{\Delta_1}\left(2S_3^{(\mathrm{dry})} + S_6^{(\mathrm{dry})} - 2S_3^0 - S_6^0\right)^2,\\
\Delta_1 &= 4S_1^{(\mathrm{dry})} + 4S_3^{(\mathrm{dry})} + S_6^{(\mathrm{dry})} + \phi\beta_{\mathrm{fl}} - (4S_1^0 + 4S_3^0 + S_6^0)(1+\phi),
\end{aligned} \tag{14}$$

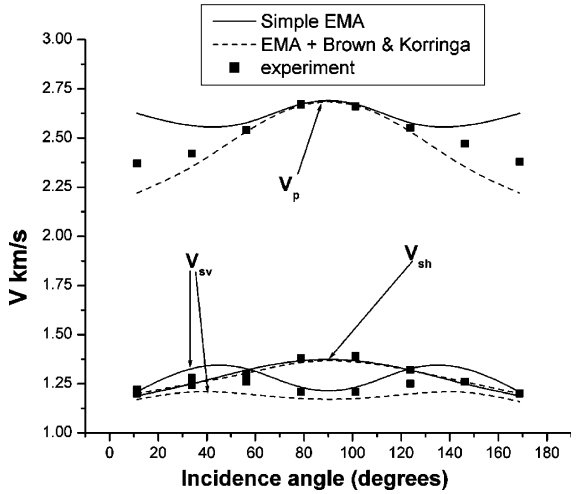

Fig. 5. Comparison of measured data (■) with the simple EMA model (solid lines) and the EMA using Gassmann and Brown & Korringa (dotted lines) method for water saturated sample, containing micro-cracks.

where

$$S_1^{(\mathrm{dry})} = \frac{C_{33}}{2\Delta_2},$$
$$S_2^{(\mathrm{dry})} = \frac{1}{C_{11} - C_{12}},$$
$$S_3^{(\mathrm{dry})} = -\frac{C_{13}}{\Delta_2},$$
$$S_5^{(\mathrm{dry})} = \frac{1}{C_{44}},$$
$$S_6^{(\mathrm{dry})} = \frac{(C_{11} + C_{12})}{\Delta_2},$$
$$\Delta_2 = 2\left(\frac{1}{2}(C_{11} + C_{12})C_{33} - C_{13}^2\right).$$

The results of calculations and the experimental data are represented in Fig. 5. The obtained results analysis indicates the good correspondence of the predictions to the experimental data for S-waves.

It is interesting to compare the predictions with the experimental data for P-waves. The experimental data are between the theoretical curves calculated by using two EMA theory variants. The obtained result is explained to that the frequency region, in which the experiments were carried out, is considerably higher than frequency region where the Brown–Korringa theory works well. At the same time the elastic wave frequency in experiments is insufficiently high to neglect the hydrodynamic effects connected with filtration. It seems to us that using of the low-frequency variant of the theory in the frequency region corresponding to seismic diapason is more correct.

5. Conclusions

Many geomaterials have anisotropy and are micro-inhomogeneous. The method to calculate effective elastic parameters of micro-inhomogeneous media, represented in this paper, is based on the self-consistent

methods ideology (the EMA model). The system of equations used in calculations is nonlinear, but its numerical solution doesn't cause any difficulty with the modern computer techniques application. This model as compared with other theoretical models, using the low concentration approximation, can be applied to more high volume concentration of inclusions.

In the case of a connected fluid-filled pores system, two calculation variants have been presented. In the low-frequency range which includes the frequency range, typical for seismic researches, it is expedient to calculate elastic properties of dry rock and use tensorial relations by Gassmann (1951) and Brown and Korringa (1975), which connect elastic module of dry and saturated porous media. In the frequency range of 1 MHz, typical for laboratory researches, it is advisable to apply direct solution of the Eq. (3) for saturated media, which fluid component shear module tends to zero. To develop the theory of effective media, containing connected pores system with movable fluid, in all frequency range it is advisable to use the theory of the mechanics of saturated porous media.

Acknowledgment

The authors are grateful to Drs. Elena Kazatchenko and Aleksandr Mousatov for their useful discussions and advise and consider as a pleasant debt to express gratitude to the Mexican Petroleum Institute, where in the framework of the scientific program "'Naturally Fractured Reservoirs" this study was fulfilled.

Appendix A. Properties of tensorial basis T

The convenience of the tensorial basis introduced by Eq. (4) is in the following properties:

1. The product of the T-basis over two indices belongs to the same basis.
2. If a certain tensor $\mathbf{H}$ is expressed in the T-basis.

$$\mathbf{H} = H_1\mathbf{T}^2 + H_2\left(\mathbf{T}^1 - \frac{1}{2}\mathbf{T}^2\right) + H_3\mathbf{T}^3 + H_4\mathbf{T}^4 + H_5\mathbf{T}^5 + H_6\mathbf{T}^6, \tag{A.1}$$

the inverse tensor $\mathbf{H}^{-1}$ is determined by the expression

$$\mathbf{H}^{-1} = \frac{H_6}{2\Delta}T^2 + \frac{1}{H_2}\left(\mathbf{T}^1 - \frac{1}{2}\mathbf{T}^2\right) - \frac{H_3}{\Delta}\mathbf{T}^3 - \frac{H_4}{\Delta}\mathbf{T}^4 + \frac{4}{H_5}\mathbf{T}^5 + \frac{2H_1}{\Delta}\mathbf{T}^6, \tag{A.2}$$

where $\Delta = 2(H_1H_6 - H_3H_4)$.

3. If two tensors $\mathbf{H}$ and $\mathbf{F}$ are given in the T-basis, then the contraction of these tensors over two indices is

$$\begin{aligned} H_{ijmn}F_{mnkl} = {} & (2H_1F_1 + H_3F_4)T^2_{ijkl} + H_2F_2\left(T^1_{ijkl} - \frac{1}{2}T^2_{ijkl}\right) + (2H_1F_3 + H_3F_6)T^3_{ijkl} \\ & + (2H_4F_1 + H_6F_4)T^4_{ijkl} + \frac{1}{2}H_5F_5T^5_{ijkl} + (H_6F_6 + 2H_4F_3)T^6_{ijkl}. \end{aligned} \tag{A.3}$$

Appendix B. One-particle problem for a spheroid in the transversely isotropic media

The tensor P introduced in Eq. (4) is the basic quantity in the solution of the one-particle problem for a spheroidal inclusion embedded in the transversely isotropic medium with tensor of elastic module L. To

obtain the explicit expressions for the components of this tensor it is necessary to calculate an integral expression over the region v occupied by the spheroidal inclusion

$$P_{ijkl} = \int_v \frac{\partial^2}{\partial x_j \partial x_l} G_{ik}(\boldsymbol{x} - \boldsymbol{x}')\mathrm{d}\boldsymbol{x}'\Big|_{(ij)(kl)}, \tag{B.1}$$

where $G(x)$ is the Green's function for a generally anisotropic unbounded medium and the symbol parenthesis () stands for the symmetrization over the corresponding indices. In the arbitrary anisotropic medium, the Green's function can be represented in the form

$$G_{ik}(\boldsymbol{x}) = \frac{1}{r}\Gamma_{ik}(\theta, \varphi), \tag{B.2}$$

where (r, θ, φ) is the spherical coordinate system.

Applying the approach developed by Vaculenko (1998), Eq. (B.1) can be transformed in the surface integral over a unit sphere Ω

$$\mathbf{P} = \mathbf{E} \cdot \int_\Omega (\mathbf{e}^r \cdot \mathbf{E} \cdot \mathbf{e}^r)^{-1} \mathbf{e}^r (\nabla^* \boldsymbol{\Gamma}(\mathbf{e}^r) - \boldsymbol{\Gamma}(\mathbf{e}^r)\mathbf{e}^r)\mathrm{d}\Omega, \tag{B.3}$$

where $\mathbf{e}^r$, $\mathbf{e}^\theta$, $\mathbf{e}^\varphi$ are the basis vectors of the spherical coordinate system and

$$\nabla^* = \frac{\mathbf{e}^\varphi}{\sin\theta}\frac{\partial}{\partial\varphi} + \mathbf{e}^\theta \frac{\partial}{\partial\theta}. \tag{B.4}$$

In Eq. (B.3), the second rank tensor $\mathbf{E}$ depends on the inclusion form and it is defined by the following expression

$$E_{ij} = \frac{1}{\alpha_1^2} e_i^1 e_j^1 + \frac{1}{\alpha_2^2} e_i^2 e_j^2 + \frac{1}{\alpha_3^2} e_i^3 e_j^3, \tag{B.5}$$

where e^1, e^2, e^3 are the unit vectors of ellipsoid symmetry axes, and α_1, α_2, α_3 are the ellipsoid semi-axes.

Taking into account that the medium is transversely isotropic, it is convenient to find the integral (B.3) in the system of cylindrical coordinates. For this purpose, tensors $\boldsymbol{\Gamma}$and $\mathbf{E}$ should be rewritten as the functions of ρ, φ, z coordinates.

Tensor $\boldsymbol{\Gamma}(\boldsymbol{\theta})$ and its components for the elastic field in a transversely isotropic medium have been obtained explicitly (Kröner, 1953) and the result was corrected by Yoo (1974). Thus,

$$\Gamma_{ik}(\theta, \varphi) = \Gamma_{\varphi\varphi}(\theta) e_i^\varphi e_k^\varphi + \Gamma_{\rho\rho}(\theta) e_i^\rho e_k^\rho + \Gamma_{\rho z}(\theta)(e_i^\rho e_k^z + e_i^z e_k^\rho) + \Gamma_{zz}(\theta) e_i^z e_k^z, \tag{B.6}$$

$$\begin{aligned}
&\Gamma_{\varphi\varphi}(\theta) = \sum_{l=1}^{3} \frac{(b_l - a_l\gamma_l)\sin^2\theta - a_l\cos^2\theta}{\sin^2\theta\sqrt{\gamma_l\sin^2\theta + \cos^2\theta}}, \quad \Gamma_{\rho\rho}(\theta) = \sum_{l=1}^{3} \frac{b_l\sin^2\theta + a_l\cos^2\theta}{\sin^2\theta\sqrt{\gamma_l\sin^2\theta + \cos^2\theta}}, \\
&\Gamma_{\rho z}(\theta) = \sum_{l=1}^{3} \frac{c_l\cos\theta}{\sin\theta\sqrt{\gamma_l\sin^2\theta + \cos^2\theta}}, \quad \Gamma_{zz}(\theta) = \sum_{l=1}^{3} \frac{d_l}{\sqrt{\gamma_l\sin^2\theta + \cos^2\theta}},
\end{aligned} \tag{B.7.1–4}$$

where coefficients a_l, b_l, c_l, d_l and γ_1, γ_2, γ_3 depend on the components of the tensor of the elastic moduli and these coefficients can be represented using Voight's matrix

$$a_l = \frac{1}{f_l}[(C_{66} - C_{11})(C_{33} - \gamma_l C_{44}) + (C_{13} + C_{44})], \tag{B.8}$$

$$b_l = \frac{1}{f_l}[(C_{44} - \gamma_l C_{11})(C_{33} - \gamma_l C_{44}) + \gamma_l (C_{13} + C_{44})], \tag{B.9}$$

$$c_l = \frac{1}{f_l}(C_{13} + C_{44})(C_{44} - \gamma_l C_{66}), \tag{B.10}$$

$$d_l = \frac{1}{f_l}(C_{44} - \gamma_l C_{11})(C_{44} - \gamma_l C_{66}), \tag{B.11}$$

$$f_l = 4\pi C_{11} C_{44} C_{66} \prod_{\substack{j=1 \\ (j \neq l)}}^{3} (\gamma_j - \gamma_l), \tag{B.12}$$

$$\gamma_1 = \frac{C_{44}}{C_{66}}, \tag{B.13}$$

where γ_2, γ_3 are the roots of the quadratic equation,

$$C_{11}C_{44}\gamma^2 + ((C_{13})^2 + 2C_{13}C_{44} - C_{11}C_{33})\gamma + C_{33}C_{44} = 0. \tag{B.14}$$

In formulas (B.6), the basis vectors of cylindrical coordinates system $\boldsymbol{e}^{\rho}$, $\boldsymbol{e}^{\varphi}$, $\boldsymbol{e}^{z}$ are

$$e^{\rho} = \begin{pmatrix} \cos\varphi \\ \sin\varphi \\ 0 \end{pmatrix}, \quad e^{\varphi} = \begin{pmatrix} -\sin\varphi \\ \cos\varphi \\ 0 \end{pmatrix}, \quad e^{z} = \begin{pmatrix} 0 \\ 0 \\ 1 \end{pmatrix}. \tag{B.15}$$

Using the relationships between the basis vectors for spherical and cylindrical coordinate systems

$$\boldsymbol{e}^{r} = \boldsymbol{e}^{\rho}\sin\theta + \boldsymbol{e}^{z}\cos\theta, \quad \boldsymbol{e}^{\theta} = \boldsymbol{e}^{\rho}\cos\theta - \boldsymbol{e}^{z}\sin\theta, \tag{B.16}$$

one can rewrite the operator ∇^* in the form

$$\nabla^* = \frac{\boldsymbol{e}^{\rho}}{\sin\theta}\frac{\partial}{\partial\varphi} + (\boldsymbol{e}^{\rho}\cos\theta - \boldsymbol{e}^{z}\sin\theta)\frac{\partial}{\partial\theta}. \tag{B.17}$$

Assuming that the inclusion is a spheroid ($\alpha_1 = \alpha_2 = \alpha$, α_3) with semi-axis α_3 parallel to the x_3-axis, we obtain

$$E_{ij} = \frac{1}{\alpha^2}(\theta_{ij} + \xi^2 e_i^z e_j^z), \tag{B.18}$$

$$\mathbf{e}^{r} \cdot \mathbf{E} \cdot \mathbf{e}^{r} = \frac{1}{\alpha^2}(\sin^2\theta + \xi^2\cos^2\theta), \tag{B.19}$$

where $\theta_{ij} = \delta_{ij} - e_i^z e_j^z$ is the orthogonal projector on the isotropy plane, and ξ is the aspect ratio.

Expressions (B.5)–(B.19) allow separate integration over the angles ϕ and θ in the Eq. (B.3). Taking into account that

$$\int_0^{2\pi} e_i^{\varphi} e_j^{\varphi} \mathrm{d}\varphi = \int_0^{2\pi} e_i^{\rho} e_j^{\rho} \mathrm{d}\varphi = \pi\theta_{ij}, \tag{B.20}$$

$$\int_0^{2\pi} e_i^{\rho} e_j^{\rho} e_k^{\rho} e_l^{\rho} \mathrm{d}\varphi = \frac{\pi}{4}(\theta_{ij}\theta_{kl} + \theta_{ik}\theta_{lj} + \theta_{il}\theta_{kj}), \tag{B.21}$$

$$\int_0^{2\pi} e_i^{\rho} e_j^{\rho} e_k^{\varphi} e_l^{\varphi} \mathrm{d}\varphi = \frac{\pi}{4}(3\theta_{ij}\theta_{kl} - \theta_{ik}\theta_{lj} - \theta_{il}\theta_{kj}) \tag{B.22}$$

we obtain after the φ-integration and applying the T-basis (Appendix A)

$$P_{ijkl} = \sum_{l=1}^{3} \int_0^{\pi} P_{ijkl}^{(l)}(\theta) \sin\theta \,\mathrm{d}\theta, \tag{B.23}$$

where

$$\begin{aligned} P_{ijkl}^{(l)}(\theta) = -\frac{\pi}{2\Delta_l}\Big\{ & (b_l - \gamma_l a_l)\gamma_l \sin^2\theta T_{ijkl}^2 + (2b_l - \gamma_l a_l) a_l \sin^2\theta \left(T_{ijkl}^1 - \frac{1}{2} T_{ijkl}^2 \right) \\ & + c_l\gamma_l(\sin^2\theta - \xi^2\cos^2\theta)(T_{ijkl}^3 + T_{ijkl}^4) + (2\xi^2(2b_l - \gamma_l a_l)\cos^2\theta \\ & - 2c_l\gamma_l(\sin^2\theta - \xi^2\cos^2\theta) + 2d_l\gamma_l\sin^2\theta) T_{ijkl}^5 + 4d_l\xi^2\cos^2\theta T_{ijkl}^6 \Big\}, \end{aligned} \tag{B.24}$$

$$\Delta_l = (\gamma_l \sin^2\theta + \cos^2\theta)^{3/2}(\sin^2\theta + \xi^2\cos^2\theta). \tag{B.25}$$

Finally, the integration in (B.23) over the angle leads to formulas (7) and (8) in the text, in which

$$J_1^{(l)} = \gamma_l \int_{-1}^{1} \frac{(1-u^2)\,\mathrm{d}u}{[1 + (\xi^2 - 1)u^2][\gamma_l + (1-\gamma_l)u^2]^{3/2}} = 2\lambda_l^2 \left[1 - \xi^2\gamma_l\lambda_l \ln\left(\frac{\lambda_l + 1}{\lambda_l - 1} \right) \right], \tag{B.26}$$

$$J_2^{(l)} = \int_{-1}^{1} \frac{u^2\,\mathrm{d}u}{[1 + (\xi^2 - 1)u^2][\gamma_l + (1-\gamma_l)u^2]^{3/2}} = 2\lambda_l^2 \left[\frac{1}{2}\lambda_l \ln\left(\frac{\lambda_l + 1}{\lambda_l - 1} \right) - 1 \right], \tag{B.27}$$

$$\lambda_l = \sqrt{\frac{1}{1 - \gamma_l\xi^2}}. \tag{B.28}$$

The components of the tensor P for cylindrical inclusions are:

$$P_{ijkl} = -\frac{1}{4C_{11}^0} T_{ijkl}^2 + -\frac{1}{4}\left(\frac{1}{C_{11}^0} - \frac{1}{C_{66}^0} \right)\left(T_{ijkl}^1 - \frac{1}{2} T_{ijkl}^2 \right) - \frac{1}{2C_{44}^0} T_{ijkl}^5. \tag{B.29}$$

References

Anderson, D.L., Minster, B., Cole, D., 1974. The effect of oriented cracks on seismic velocities. J. Geophys. Res. 79, 4011–4015.

Berge, P.A., Berryman, J.G., Bonner, B.P., 1993. Influence of microstructure on rock elastic properties. Geophys. Res. Lett. 20, 2619–2622.

Berryman, J.G., 1980. Long wavelength propagation in composite elastic media. J. Acoust. Soc. Am. 68, 1809–1831.

Berryman, J.G., 1992. Single-scattering approximations for coefficients in Biot's equations of poroelasticity. J. Acoust. Soc. Am. 91, 551–571.

Biot, M.A., 1962. Mechanics of deformation and acoustic propagation in porous media. J. Appl. Phys. 33, 1482–1498.

Brown, R., Korringa, J., 1975. On the dependence of the elastic properties of a porous rock on the compressibility of the pore fluid. Geophysics 40, 608–616.

Budiansky, B., O'Connell, R.J., 1976. Elastic module of a cracked solid. Int. J. Solid Struct. 12, 81–97.

Cheng, C.H., 1993. Crack models for a transversally isotropic medium. J. Geophys. Res. 98, 675–684.

Eshelby, J.D., 1957. The determination of the elastic field of an ellipsoidal inclusion and related problems. Proc. R. Soc. Lond. A 241, 376–396.

Gassmann, F., 1951. Über die Elastisität poroser medien. Vierteljahrsschrift der Naturf. Gesellschaft in Zurich 96, 1–23.

Gurevich, B., Sadovnicnaja, A.P., Lopatnikov, S.L., S.A, 1998. Scattering of a compressional wave in a poroelastic medium by an ellipsoidal inclusion. Geophys. J. Int. 133, 91–103.

Hoenig, A., 1979. Elastic moduli of the non-randomly cracked body. Int. J. Solids Struct. 15, 137–154.

Hornby, B.E., Shwartz, L.M., Hudson, J.A., 1994. Anisotropic effective-medium modeling of elastic properties of shales. Geophysics 59 (10), 1570–1583.

Hudson, J.A., 1980. Overall properties of a cracked solid. Math. Proc. Cambridge Philosoph. Soc. 88, 371–384.

Hudson, J.A., 1981. Wave speed attenuation of elastic waves in materials containing cracks. Geophys. J. R. Astron. Soc. 64, 133–150.

Hudson, J.A., 1990. Overall elastic properties of isotropic materials with arbitrary distribution of circular cracks. Geophys. J. R. Astron. Soc. 102, 465–469.

Hudson, J.A., Liu, E., Crampin, S., 1996. The mechanical properties of materials with interconnected cracks and pores. Geophys. J. Int. 124, 105–112.

Hudson, J.A., Pointer, Y., Liu, E., 2001. Effective-medium theories for fluid-saturated materials with aligned cracks. Geophys. Prosp. 49, 509–522.

Jacobsen, M., Hudson, J.A., Minshull, T.A., Singh, S.C., 2000. Elastic properties of hydrate-bearing sediments using effective medium theory. J. Geophys. Res. 105, 561–577.

Kachanov, M., 1992. Effective elastic properties of cracked solids: critical review of some basic concepts. Appl. Mech. Rev. 45, 304–335.

Kanaun, S.K., Levin, V.M., 1994. Effective field method in mechanics of matrix composite materials. In: Markov, K.Z. (Ed.), Advances in Mathematical Modeling of Composite Materials. World Scientific, Singapore, pp. 1–58.

Korringa, J., Brown, R.J.S., Thompson, D.D., Runge, R.J., 1979. Self-consistent imbedding and the ellipsoidal model for porous rocks. J. Geophys. Res. 84, 5591–5598.

Kröner, E., 1953. Das Fundamental integral der anisotropen elastischen Differential gleichungen. Zeitschrift für Physik 136, 402–410.

Kunin, I.A., 1983. Elastic Media with Microstructure, vol. 2. Springer, Berlin, 269 p.

Laws, N., Brockenbrouth, J.R., 1987. The effect of micro-crack systems on the loss of stiffness of brittle solids. Int. J. Solids Struct. 23, 1247–1268.

Lin, S., Mura, T., 1973. Elastic fields of inclusions in anisotropic media. Phys. Status Solidi (a) 15, 281–285.

Markov, M., Kazatchenko, E., Mousatov, A., 2003. Joint Inversion of Acoustic and Resistivity Data for Carbonate Microstructure Evaluation SPWLA 44th Annual Meet. Paper, Y.

Mavko, G., Mukeri, T., Dvorkin, J., 1998. The Rock Physics Handbook. Tools for Seismic Analysis in Porous Media. Cambridge University Press, 330p.

Milton, G.W., 1985. The coherent potential approximation is a realizable effective medium scheme. Commun. Math. Phys. 99, 463–500.

Norris, A., 1985. A differential scheme for the effective moduli of composites. Mech. Mater. 4, 1–16.

Nur, A., 1971. Effect of stress on velocity anisotropy in rocks with cracks. J. Geophys. Res. 76, 2022–2034.

O'Connell, R.J., Budiansky, B., 1974. Seismic velocities in dry and saturated cracked solids. J. Geophys. Res. 79, 5412–5426.

Peacock, S., Hudson, J.A., 1990. Seismic properties of rock with distributions of small cracks. Geophys. J. Int. 102, 471–484.

Rathore, J.S., Ejaer, E., Holt, R.M., Renlie, L., 1994. P- and S-wave anisotropy of a synthetic sandstone with controlled crack geometry. Geophys. Prosp. 43, 711–728.

Sayers, C.M., Kachanov, M., 1991. A simple technique for finding effective elastic constants of cracked solids for arbitrary crack orientation statistics. Int. J. Solids Struct. 27, 671–680.

Sevostianov, I., Yilmaz, N., Kushch, V., Levin, V., 2004. Effective elastic properties of matrix composites with transversely-isotropic phases. Int. J. Solids Struct., this issue.

Sheng, P., 1991. Consistent modeling of the electrical and elastic properties of sedimentary rocks. Geophysics 56, 1236–1243.

Thomsen, L., 1995. Elastic anisotropy due to aligned cracks in porous rocks. Geophys. Prosp. 43, 805–829.

Vaculenko, A.A., 1998. On the effective properties and strength of ceramic composites. Mech. Solids 6, 50–71.

Xu, S., 1998. Modelling the effect of fluid communication on velocities in anisotropic porous rocks. Int. J. Solids Struct. 35, 4685–4707.

Yoo, M.H., 1974. Elastic interaction of small defects and defect clusters. Phys. Stat. Sol. (b) 61, 411–418.